Discovery of a Self-healing Catalyst for the Hydrolytic Dehydrogenation of Ammonia Borane

F. Pelin Kinik,[1] Tu N. Nguyen,[1] Emad Oveisi,[2] Bardiya Valizadeh,[1] Fatmah Mish Ebrahim,[1] Andrzej Gładysiak,[1] Mounir Mensi[3] and Kyriakos C. Stylianou[1]*

1. Laboratory for Molecular Simulation (LSMO), Institute of Chemical Sciences and Engineering, École Polytechnique Fédérale de Lausanne (EPFL Valais), Rue de l'Industrie 17, 1951 Sion, Switzerland.

2. Interdisciplinary Center for Electron Microscopy, École Polytechnique Fédérale de Lausanne (EPFL), 1015 Lausanne, Switzerland.

3. Institute of Chemical Sciences and Engineering, École Polytechnique Fédérale de Lausanne (EPFL Valais), Rue de l'Industrie 17, 1951 Sion, Switzerland.

Abstract

Sustainable catalysts based on earth-abundant elements are considered as economical alternatives to precious-metal-bearing catalysts and could be impactful for many applications. Self-healing sustainable catalysts, which in addition to their 'green' characteristic can spontaneously repair themselves without the need of applying heat, pressure or electrochemical bias, are particularly desirable for numerous large-scale chemical processes. Herein, we present the discovery of such a catalyst, named **SION-X**, for the hydrolytic dehydrogenation of ammonia borane (AB, NH_3BH_3). **SION-X**, with the chemical formula of $Cu^{II}_2[(BO)(OH)_2](OH)_3$, is the synthetic form of the mineral Jacquesdietrichite and, following in situ reduction, catalyzes the release of almost all 3 equivalents of hydrogen (H_2) from 1 equivalent of AB. During the reaction, the Cu^{II} ions in **SION-**

X are reduced to Cu^0 nanoparticles, and after the reaction, following exposure to air, they are oxidized re-forming **SION-X**. As a consequence, the catalytic activity of **SION-X** toward the production of H_2 from AB remains unchanged over many cycles. The self-healing catalysis of **SION-X** in the absence of any extra energy input gives a new perspective in heterogeneous catalysis for energy-related applications.

1. Introduction

Hydrogen (H_2) is a clean and renewable energy carrier, and is considered as an ideal candidate for future mobile and stationary applications.[1] For large-scale utilization of H_2 energy, safe and efficient storage and release of H_2 are of great importance and still remain a challenging task to achieve.[2] Different hydrogen storage systems such as sorbent materials, metal hydrides, and complex hydrides have been investigated to overcome these challenges.[3-7] In recent years, boron-nitrogen-based (B-N) hydride compounds such as ammonia borane (AB, NH_3BH_3), have drawn attention due to their capability of storing and releasing significant quantities of H_2.[8,9] While most B-N based compounds such as hydrazine borane ($N_2H_4BH_3$) or metal borohydrides such as sodium borohydride ($NaBH_4$) and lithium borohydride ($LiBH_4$) suffer from self-hydrolysis in water, AB, being the simplest B-N compound, has a high H_2 content (19.5 wt%), low molecular weight (30.9 g mol^{-1}), non-toxic nature, and particularly high stability in both aqueous solutions and air.[10] Therefore, AB has a great potential for practical on-board applications in transportation. The release of H_2 from AB can be achieved either from thermolysis or solvolysis; the latter can be further classified into hydrolysis and methanolysis, in which the dehydrogenation reaction occurs in water or methanol, respectively.[11] So far, hydrolysis has been the most benign method to obtain all 3 equivalents of H_2 from 1 equivalent of AB without the need of elevated temperatures or toxic solvents, although a catalyst is often required.[12]

The hydrolytic dehydrogenation of AB can be catalyzed by a wide range of catalysts, from monometallic noble metal nanoparticles (NPs) such as Ru,[13] Rh,[14] Pt,[15] Ag,[16] and Pd NPs,[17] monometallic earth-abundant transition metal NPs such as Cu,[18] Ni,[19] Co,[20] and Fe NPs,[21] bimetallic/multimetallic NPs such as RuRh,[22] RuCo,[23] CuCoMo,[24] and RuCuCo NPs,[25] NPs of transition metal oxides such as Cu_2O[26] and phosphides such as Ni_2P[27,28] and CoP,[29,30] to transition metal complexes such as an iridium pincer complex.[31] While these catalysts are quite efficient, they suffer from the following disadvantages: *i.* the noble-metal-based catalysts are expensive, non-sustainable, and impracticable for large-scale applications, *ii.* most non-noble-metal catalysts are air sensitive and can be easily oxidized, thus require special handling and storage, and are sometimes difficult to regenerate, and *iii.* the catalytic activity is partially decreased or even completely disabled after few cycles of the reaction (e.g. in earth-abundant transition metals).[26] Although capping agents have been used for the stabilization of metal NPs, they lack long-term stability under harsh reaction conditions. Moreover, there are some debates that capping agents may act as a "poison" during the reaction, limiting the accessibility of active sites.[32] Taking these drawbacks into consideration, the goal of the present work is to develop new sustainable catalysts that are based on earth-abundant elements, are air stable, and can be easily regenerated, stored and handled for the hydrolytic dehydrogenation of AB. In terms of regeneration, self-healing, which is the ability of the catalyst to spontaneously repair itself during normal operations, is the most attractive approach and highly important for practical applications since the catalyst stability is vital for economic viability.[33] It should be emphasized that the self-healing mechanism is different from the recyclability or stability of the catalyst. Although most of the heterogeneous catalysts can be re-used for a certain number of cycles, each catalyst has a finite lifetime which could vary from seconds to years. After the catalyst loses its activity due to several reasons, it should be either

regenerated or replaced. The regeneration/replacement of the catalyst requires the shutdown of the process and the disruption of the production, which costs billions of dollar per year for the industry.[34] Therefore, the self-healing mechanism counts as a highly desired property in economical point of view.

Herein, we report a novel self-healing sustainable catalyst that can efficiently produce H_2 from AB. Our catalyst, $Cu_2[(BO)(OH)_2](OH)_3$ (**SION-X**), is the synthetic form of the Jacquesdietrichite mineral which was found in the Tachgagalt mine in Morocco in 1999.[35] **SION-X** was first obtained as a blue powder when the residue of the reaction between the Cu-bpy-Cl metal-organic framework (MOF) and AB was left in open air. When **SION-X** (26.7 mol%) was employed for the hydrolysis of AB, more than 90% conversion ($\geq$ 2.7 equivalents) of H_2 was obtained in ~ 45 mins, during which it transformed to Cu^0 NPs. When the reaction mixture was then exposed to air, the blue powder of **SION-X** was self-healed and reformed from Cu^0 NPs in quantitative yield. We performed 10 cycles of catalysis-regeneration during which the activity of **SION-X** remained unchanged. This self-healing catalysis, in which the catalyst can restore its structural integrity in open air without applying heat, pressure or electrical bias, is of great importance for prolonging the lifetime of the catalyst. This kindles the potential use of **SION-X** for the hydrolytic dehydrogenation of AB on a large-scale. Below, we delineate the discovery of **SION-X** from the reaction between the Cu-bpy-Cl and AB, analyze its performance for the generation of H_2, and discuss its transformation during the hydrolysis reaction.

2. Experimental

2.1. Materials synthesis

All chemicals were purchased from commercial suppliers and used without any further purification: copper (I) chloride (Sigma Aldrich), copper (I) bromide (Sigma Aldrich), copper (I)

iodide (Sigma Aldrich), 4,4´-bipyridyl (TCI Chemicals), ammonia borane (AB, Sigma Aldrich), acetonitrile (Merck) and diethyl ether (Sigma Aldrich).

The Cu-bpy-Y (Y: Cl, Br, I) materials were synthesized based on reported protocols.[36,37] The addition of 4,4´-bpy (5.0, 0.13 and 0.21 mmol, respectively) in acetonitrile to the solution of Cu-Y salt (5.0, 0.13 and 0.11 mmol, respectively) in acetonitrile resulted in the immediate formation of a dark red solid for Cu-bpy-Cl and Cu-bpy-Br while orange-red plates were observed for Cu-bpy-I. The powders were filtered and washed with ethanol (3×20 ml) followed by diethyl ether (3×20 ml). Finally, the as-synthesized MOFs were dried at room temperature under ambient conditions. For the formation of **SION-X**, 14.8 mg (0.058 mmol) of Cu-bpy-Cl was dispersed in 15.0 ml of Millipore water and the suspension was sonicated for 20 minutes to provide a uniform distribution of the MOF powder in water. Then, 10.0 mg (0.324 mmol) of AB was dissolved in 5.0 ml of Millipore water and added to the suspension. The solution was exposed to open atmosphere and stirred gently overnight at room temperature under ambient conditions. First, Cu-bpy-Cl started to collapse (since AB is a reducing agent) and Cu^0 NPs were formed. Meanwhile, some of AB introduced in the solution was hydrolytically dehydrogenated simultaneously; therefore, NH_4^+ and BO_2^- ions were released in the solution. The BO_2^- ions in the solution, Cu^0 NPs which were derived from the MOF, and the O_2 molecules in the air combined and formed **SION-X**, $Cu_2[(BO)(OH)_2](OH)_3$. The blue solid was collected and washed with Millipore water several times, then dried in air at room temperature. Following the same procedure, **SION-X** can be synthesized in gram-scale when grams of Cu-bpy-Cl are used.

2.2. Hydrolytic dehydrogenation of AB

The hydrolysis experiments were performed in a 25.0 ml Pyrex glass reactor, at room temperature under vigorous mixing. In a typical experiment, a molar ratio between the catalyst and AB (the

optimum conditions for Cu-bpy-Y: catalyst/AB = 0.1, for **SION-X**: catalyst/AB = 0.27) was determined and the catalyst was suspended in 9.0 ml of Millipore water. Then, the suspension was sonicated and purged with nitrogen for 20 min under gentle stirring, to remove the dissolved oxygen. In a separate vial, 6 mg of AB was dissolved in 1 ml of Millipore water and injected in the reaction solution. During the reaction, the solution was continuously stirred at a stirring speed of 750 rpm in order to eliminate any mass transfer limitation effects.[38,39] When the reaction is complete, 200 µl of the gaseous product was abstracted from the head-space and analyzed by gas chromatography (PerkinElmer Clarus 480 GC, N_2 carrier gas), equipped with a thermal conductivity detector and a molecular sieve 5 Å column. The hydrolysis of AB takes place based on the following equation:

$$NH_3BH_3 + 2H_2O \rightarrow NH_4^+ + BO_2^- + 3H_2 \quad (1)$$

where ~3 equivalents of H_2 per NH_3BH_3 can be produced at ambient temperature in the presence of a suitable catalyst.

Recycling experiments were performed for the **SION-X** using the optimized molar ratio of **SION-X**/AB = 0.27, which involved 10 catalytic runs, each for ~45 minutes. At the end of each cycle, the septum was first removed from the Pyrex glass reactor to remove the generated hydrogen from the previous run. Then, the reactor was exposed to the open atmosphere overnight under vigorous mixing to enable the transformation of Cu^0 NPs into the **SION-X**. To ensure the formation of the **SION-X** at the end of each run, the blue powder occurred in the solution was collected and dried, and its PXRD pattern was recorded. The obtained **SION-X** was again suspended into the Millipore water, purged with N_2, then fresh AB solution was added to the reactor and the H_2 evolution was recorded.

3. Results and discussion

Cu-bpy-Y MOFs (Figure 1a,b) are 2-dimensional networks that were first synthesized by Yaghi *et al.* in 1995 (for the Cl analogue)[36] and then by Batten and coworkers.[37] These MOFs can be easily synthesized in gram-scale quantities with high yield (94%) just after the ligand and metal solutions are mixed together at room temperature. This is a rare case since high temperature and pressure is usually required for MOF synthesis. To investigate the catalytic activity of these MOFs toward the hydrolytic dehydrogenation of AB,[40] each of Cu-bpy-Y was first dispersed in Millipore water in a glass reactor, and the dispersion was then sonicated and degassed with nitrogen gas. The AB aqueous solution was next added to the reactor and the H_2 production was analyzed by gas chromatography. Among these MOFs, Cu-bpy-Br produced ~1.5 equivalents of H_2 from AB (~50% conversion in 3 hours) while Cu-bpy-Cl and Cu-bpy-I showed ~ 35% and ~10% H_2 conversion after 3 hours, respectively (Figure 1c). When shorter-time reactions were performed, it was found via powder X-ray diffraction (PXRD) that the Cu-bpy-Cl completely collapsed after 20 mins, and new Bragg reflections corresponding to a mixture of Cu^0, Cu_2O, and CuO NPs appeared. The formation of Cu^0 NPs is expected since AB is an efficient reducing agent leading to the structural collapse of Cu-bpy-Cl.[40] It is thought that the formation of both Cu_2O and CuO NPs occurred due to the oxidation of the surface of Cu^0 NPs when the sample was collected and dried in air.[41] As revealed by PXRD, both Cu-bpy-Br and Cu-bpy-I retained their structural integrities after 3 hours of AB hydrolysis but small Bragg reflections of Cu^0, Cu_2O, and CuO appeared in the powder patterns of bulk powders (Figure S1-3, Supporting Information). The X-ray photoelectron spectroscopy (XPS) data collected on Cu-bpy-Cl after 3 hours of AB hydrolysis show two components with binding energies at 932.5 and 934.5 eV corresponding to the Cu $2p_{3/2}$ core level (Figure S4, Supporting Information). These two components can be assigned to Cu^0 and/or Cu^I

(932.5 eV) and Cu^{II} (934.5 eV);[42] this observation is in agreement with the PXRD pattern of the bulk material (Figure S1, Supporting Information).

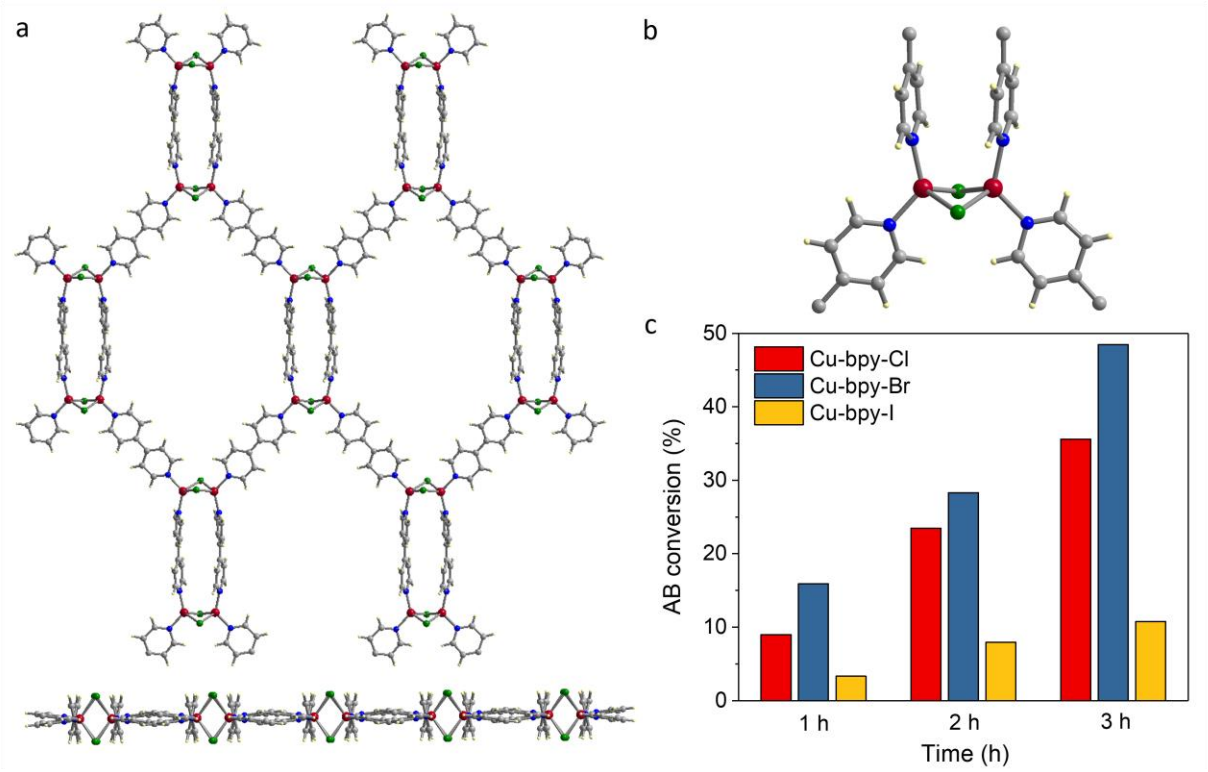

Figure 1. Cu-bpy-Y (Y= Cl, Br and I) MOFs: the relationship between morphology and catalytic activity toward AB hydrolysis. **a)** Structure representation of the isostructural 2-dimensional Cu-bpy-Y, **b)** The Cu_2-unit present in Cu-bpy-Y MOFs – each Cu^I is four-coordinated. Atom code: C: gray; N: blue; Cu: dark red; Cl/Br/I: green; H: pale yellow. **c)** The catalytic activities of Cu-bpy-Y MOFs toward hydrolytic dehydrogenation of AB at the end of 1, 2 and 3 hours**.**

To further investigate the structural changes of Cu-bpy-Y before and after the hydrolysis reaction, scanning electron microscopy (SEM) and transmission electron microscopy (TEM) images were collected. The SEM (Figure S5, Supporting Information) and high-angle annular dark-field scanning TEM (HAADF-STEM) images (Figure 2a-c) of the bulk Cu-bpy-Cl after the reaction revealed the presence of agglomerated NPs. Contrarily, the images collected on Cu-bpy-

Br and Cu-bpy-I showed that well-defined crystals are still present in the bulk material with varying amounts of NPs (Figure 2b,c and Figure S5, Supporting Information). Based on these findings, the stability of Cu-bpy-Y in AB solution follows the order of Cu-bpy-Cl < Cu-bpy-Br < Cu-bpy-I, which is in agreement with the trend of the reduction potentials of CuY ($E^0_{CuCl/Cu}$ = +0.137 V, $E^0_{CuBr/Cu}$ = +0.035 V, $E^0_{CuI/Cu}$ = -0.185 V). This is due to the decrease in electronegativity of the halogens from Cl^- to I^-, and hence the decrease in positive charge density of Cu^+ from Cu–Cl to Cu–I. Comparing the amounts of H_2 produced after 1, 2, and 3 hours by the Cu-bpy-Y reveals that the Cl-analogue generated less H_2 than the Br-analogue, although based on PXRD analysis, the former was fully reduced to metallic Cu^0 NPs, while the latter was only partially reduced, and comprised of a mix of Cu^0 NPs and MOF crystals. This observation highlights that even though Cu^0 NPs can be a good catalyst for the dehydrogenation of AB, there is a need to prevent their aggregation.[43] The presence of Cu-bpy-Br crystals after the catalytic reaction is thought to be highly advantageous as the crystals act as a support for the Cu^0 NPs, preventing their aggregation, thus leading to a higher catalytic activity toward the AB hydrolysis and H_2 generation. This observation is consistent with previous studies where supports such as graphite and others were used to immobilize metal NPs for the efficient hydrolysis of AB.[44,45]

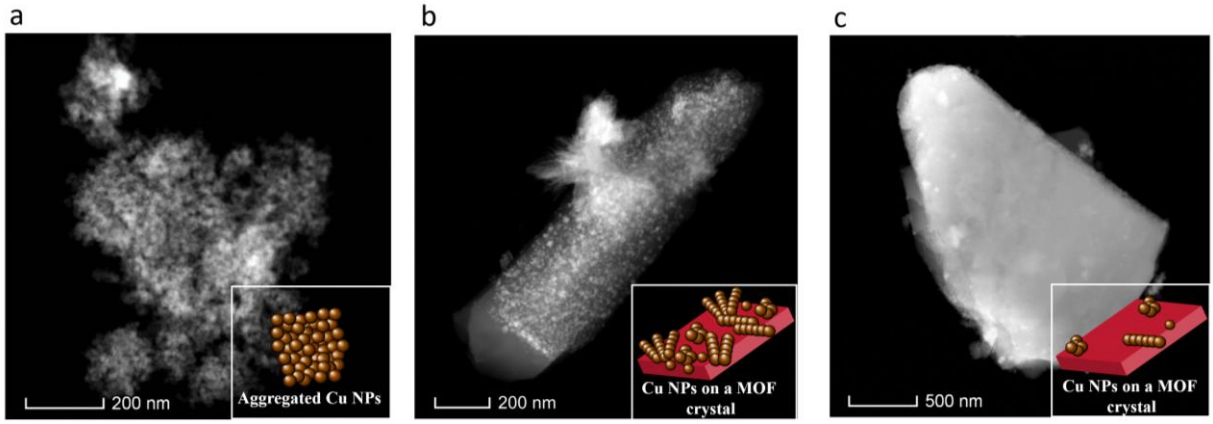

Figure 2. HAADF-STEM images of **(a)** Cu-bpy-Cl, **(b)** Cu-bpy-Br and **(c)** Cu-bpy-I after 3 hours of AB hydrolysis, respectively. Inset: the schematic representation of each structure after 3 hours.

When the brown/black residue of the reaction between Cu-bpy-Cl and AB was left in open air, without applying any heat or pressure, we observed the formation of a blue crystalline powder – **SION-X** (Figure 3a). PXRD analysis revealed that **SION-X** exhibits a pattern comparable to that of the Jacquesdietrichite mineral, with the chemical formula of $Cu_2[(BO)(OH)_2](OH)_3$ (Figure 3d). This mineral was discovered first in Morocco by the French geologist and mineralogist Jacques Emile Dietrich in 1999.[35] A synthetic analogue of Jacquesdietrichite was also reported by Behm *et al.*[46] The structural identity of **SION-X** was further confirmed by Fourier transform infrared (FTIR) spectroscopy (Figure S6, Supporting Information) and inductively coupled plasma optical emission spectrometry (ICP-OES) measurements (Figure S7, Supporting Information).

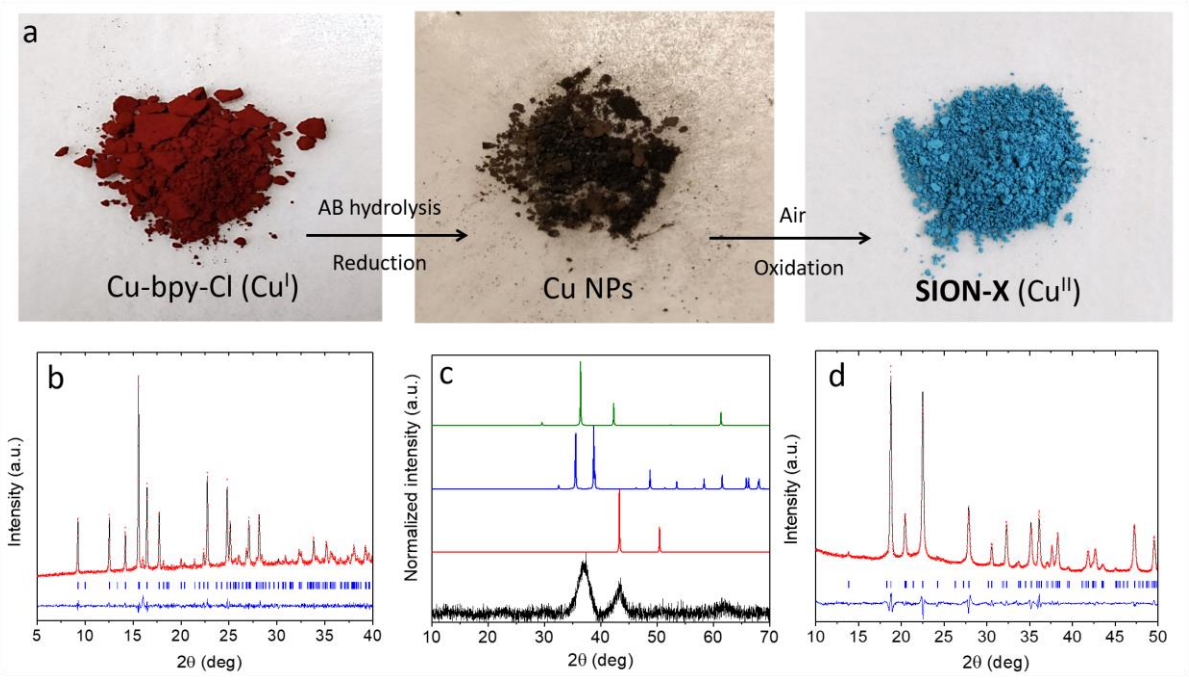

Figure 3. a) The colors of the samples (Cu-bpy-Cl, Cu NPs and **SION-X**) and the synthetic route followed for the synthesis of **SION-X** in solution environment. For the formation of **SION-X,** Cu

NPs are kept in the original reaction solution and exposed to air-oxidation overnight under continuous stirring. **b)** Le Bail fit of the PXRD pattern of Cu-bpy-Cl: a space group $I4_1/acd$: R_p = 5.19%, R_{wp} = 7.03%, a = 14.224(4) Å, c = 38.560(13) Å; λ = 1.54187 Å (experimental data: red dots, refined Le Bail profiles: solid black lines, and difference between them: solid blue line). **c)** The PXRD pattern of the bulk Cu-bpy-Cl after AB hydrolysis for 3 hours (black pattern) shows the formation of a mixture of Cu^0 (red), CuO (blue) and Cu_2O (green) NPs. **d)** Le Bail refinement of **SION-X**: space group *Pnma:* R_p = 4.73%, R_{wp} = 6.07%, a = 9.4607(7) Å, b = 5.8514(3) Å, c = 8.7001(6) Å; λ = 1.54187 Å (experimental data: red dots, refined Le Bail profiles: solid black lines, and difference between them: solid blue line).

Cu 2p XPS spectrum revealed that the bulk **SION-X** powder consisted of mostly Cu^{II} (≥ 95%) ions, confirming that Cu^0 NPs are almost quantitatively oxidized to form **SION-X** (Figure S4, Supporting Information). This observation was further verified with the XPS analysis of B 1s region for **SION-X**, resulting in a very strong B peak (Figure S8, Supporting Information). The SEM and TEM images collected on the samples Cu-bpy-Cl, Cu NPs and **SION-X** demonstrated the emergence of **SION-X** consisting of cuboid shaped single crystals (Figure 4 and Figure S9a, Supporting Information)**.** The formation of **SION-X** can be attributed to the oxidation of the Cu^0 NPs by O_2 in air, in combination with the presence of BO_2^-, which is the product resulting from the hydrolysis of AB in the reaction mixture.

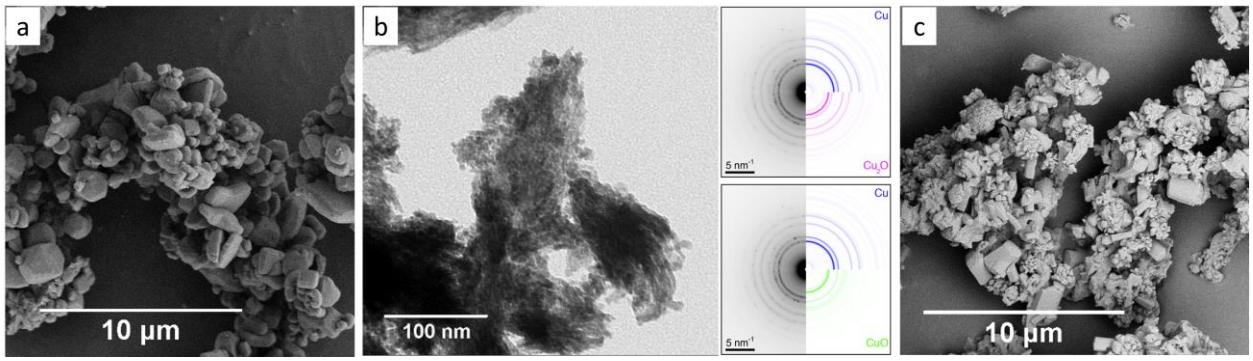

Figure 4. a) SEM image of the as-synthesized Cu-bpy-Cl shows homogeneity of the sample and that the crystal shape of Cu-bpy-Cl is based upon rectangular plates. **b)** Bright field TEM image of Cu NPs derived from Cu-bpy-Cl. Selected area electron diffraction patterns show that the brown/black powder comprises a mixture of Cu^0, CuO and Cu_2O NPs. **c)** The SEM image of as-synthesized **SION-X** confirms that crystals have cuboid shapes.

SION-X was employed toward AB hydrolysis with the aim to investigate its catalytic activity, reaction kinetics, regeneration and reusability. To optimize the amount of **SION-X** for this reaction, different molar ratios of **SION-X**/AB were tested by changing the amount of **SION-X** while the AB amount (0.1944 mmol) was kept constant (Figure 5a). For the best performance mixture with the molar ratio of **SION-X**/AB = 0.27 (where **SION-X** = 0.052 mmol**),** ~3 equivalents of H_2 were obtained after 45 minutes of reaction at 25 °C, giving a turnover frequency (TOF) of 1.85 min^{-1} (with a hydrogen generation rate of 463.2 mmol g_{cat}^{-1} h^{-1}) at <20% conversion. These values are higher than those reported for other Cu-based catalysts (used with no support) such as the commercial Cu^0 NPs (0.06 min^{-1})[41] and Cu_2O (0.18 min^{-1}),[41] and some Cu-based catalysts grown or deposited on supports such as Cu^0/γ-Al_2O_3 (0.27 min^{-1})[47] (Table S1, Supporting Information). It should be emphasized that Cu NPs derived from SION-X perform as the active catalyst without the combination with any other metal or the presence of any capping agent/support material. We additionally studied the kinetics of the hydrolysis reaction varying the amount of AB while the amount of **SION-X** was kept constant (optimized amount, 12.5 mg). The observed sigmoidal kinetic curves are characteristic of a pre-catalyst turning into the active catalyst: from **SION-X** to Cu^0 NPs (Figure S10a,b, Supporting Information). The H_2 evolution rate was then calculated and showed 0.62- and 0.7-order dependences as a function of AB and **SION-X** concentrations, respectively. The hydrolysis reaction with respect to AB concentration does not

follow the zero-order kinetics, which might be attributed to the competitive interaction between water and AB molecules with the catalyst surface.[27,48] The temperature dependence (298-318 K) of the AB hydrolysis was also studied in order to determine the activation energy (E_a) of the reaction. The values of the rate constant *k* at different temperatures were calculated from the slope of the nearly linear part of each plot (see Figure S10c, Supporting Information). From the Arrhenius plot (see inset in Figure S10c, Supporting Information), the activation energy for the hydrolytic dehydrogenation of AB catalyzed by **SION-X** was calculated to be 22.3 kJ mol^{-1}, which is lower than almost all Cu-based catalysts for AB hydrolysis, including noble catalysts such as RuCu/graphene (30.4 kJ mol^{-1}) and annealed-RGO-$Cu_{75}Pd_{25}$ (45 kJ mol^{-1}) (Table S1, Supporting Information).

During the AB hydrolysis, **SION-X** changes color and turns into brown/black suggesting that the Cu^{II} ions were reduced to Cu^0 NPs (Figure 5b,c). PXRD revealed that the composition of the bulk material after AB hydrolysis consists of Cu^0 NPs (major phase) and Cu_2O NPs. This observation is in agreement with the electron diffraction pattern, confirming the presence of both Cu^0 and Cu_2O NPs (Figure S9, Supporting Information). XPS analysis showed no noticeable B peak in the B 1s spectrum of Cu NPs (Figure S8, Supporting Information) and ICP-OES measurements revealed the presence of only trace amounts (0.218 %) of B, confirming that B cannot have a significant impact on the catalytic activity of the Cu NPs. Interestingly, when the brown/black residue was exposed in air, the blue powder was recovered, and **SION-X** was re-formed as proved by PXRD, in a quantitative yield (Figure 5d). Therefore, the fresh catalyst can be continuously regenerated. The newly obtained **SION-X** exhibited the same catalytic activity toward the hydrolytic dehydrogenation of AB. In fact, we performed 10 cycles of AB hydrolysis and catalyst regeneration and observed that the structural identity and catalytic activity of **SION-**

X remained unchanged (Figure 5e). The small differences in AB conversions between the cycles might be arising from the instrument and human errors since the injection of hydrogen into the gas chromatography (GC) was manually performed. ICP-OES analysis confirmed that negligible amount of Cu^{II} (0.0017 mol per mol of **SION-X**) is lost into the solution during the regeneration (Figure S7, Supporting Information), which corresponds to 95.75% regeneration after 50 cycles. This is a direct proof of self-healing catalysis as the catalyst can be used and regenerated for many cycles without losing performance and material; this is a key characteristic for large-scale processes where the main issue lies in catalyst deactivation over time. After the self-healing of **SION-X** from Cu NPs occurs at the end of the cycle, the same solution can be kept and fresh AB solution can be fed to restart the hydrolysis, which can eliminate the solid-liquid separation and any "off" period during the reaction. The formation of **SION-X** also provides an easy handling of the active catalyst – Cu^0 NPs, since their oxidation under open atmosphere can be eliminated without using any capping agent or support materials. It is worth noting that the term of self-healing catalysis was proposed by Nocera and co-workers for their studies on electrocatalytic water-splitting catalysis.[49,50] These earth-abundant catalysts could be self-healed in the presence of phosphate or borate anions, as the self-healing process requires less energy than that needed for the oxidation of water to O_2. In the present study, our **SION-X** catalyst is self-healed in air without the need of any extra energy input and therefore represents a new class of self-healing catalysts.

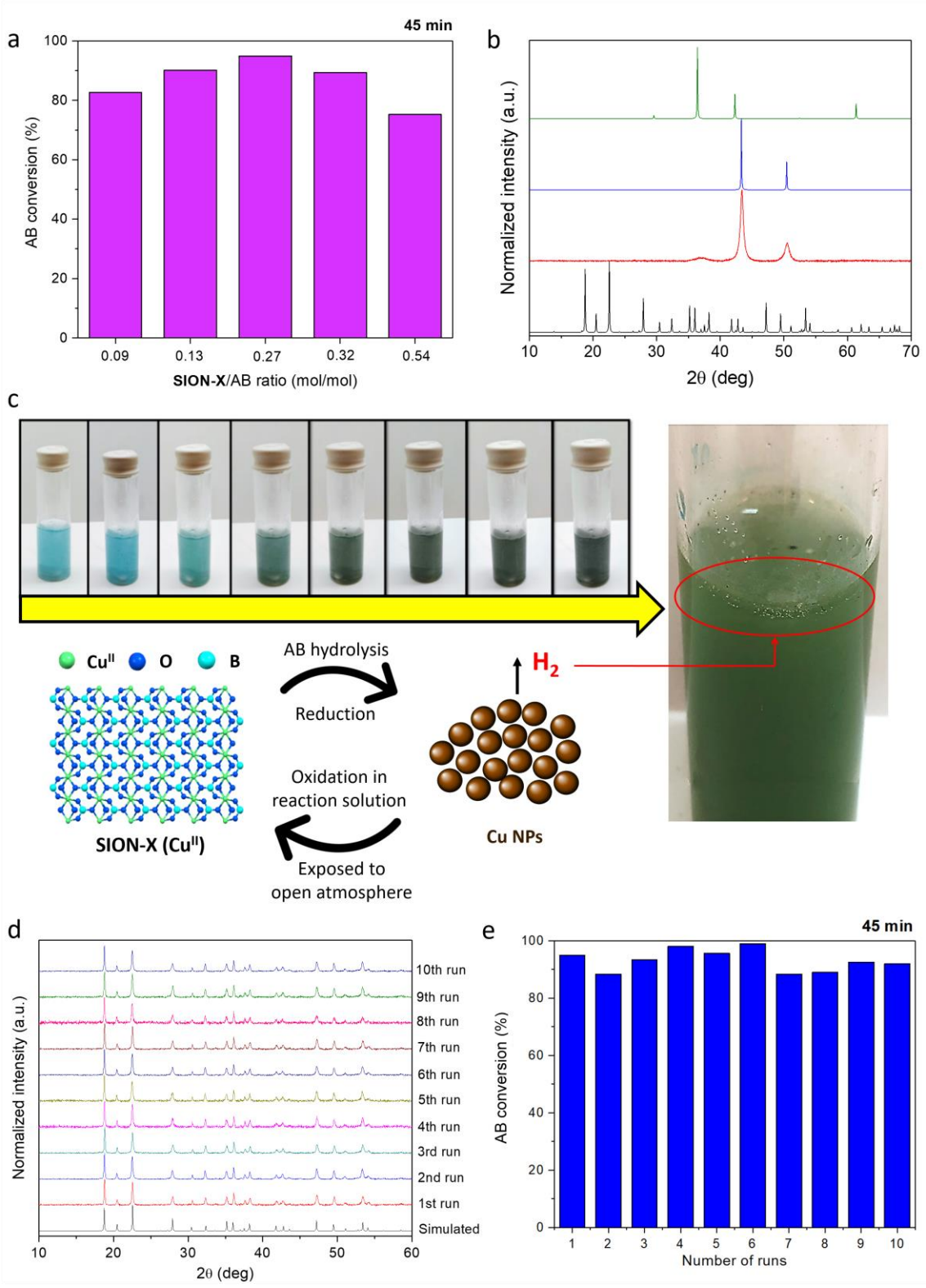
a
45 min
AB conversion (%)
SION-X/AB ratio (mol/mol)
0.09
0.13
0.27
0.32
0.54
b
Normalized intensity (a.u.)
2θ (deg)
c
Cu^II
O
B
SION-X (Cu^II)
AB hydrolysis
Reduction
Oxidation in reaction solution
Exposed to open atmosphere
H2
Cu NPs
d
Normalized intensity (a.u.)
10th run
9th run
8th run
7th run
6th run
5th run
4th run
3rd run
2nd run
1st run
Simulated
2θ (deg)
e
45 min
AB conversion (%)
Number of runs

Figure 5. a) Optimization of the amount of **SION-X** toward AB hydrolysis. **b)** PXRD pattern of the bulk material derived from **SION-X** after AB hydrolysis (red) in comparison with the patterns of **SION-X** (black), Cu^0 (blue) and Cu_2O (green) NPs. **c)** Schematic representation of the AB hydrolysis reaction: start – **SION-X** (blue solution) and end – Cu^0 NPs (brown/black solution) of the reaction. The enlarged image shows the production of H_2 bubbles by the Cu^0 NPs. **d)** PXRD patterns of **SION-X** collected after each AB hydrolysis cycle, showing the stability of the catalyst during the regeneration process. **e)** Reusability of **SION-X** as catalyst for the hydrolysis of AB for at least 10 cycles.

Although **SION-X** was prepared from Cu-bpy-Cl as the starting material, the mineral can be also synthesized based on the procedure reported by Behm *et al.*, in which the blue crystalline powder of $Cu_2[(BO)(OH)_2](OH)_3$ is obtained after mixing and stirring the aqueous solutions of $NaB(OH)_4 \cdot 2H_2O$ with $CuCl_2$ for several days at elevated temperature. These synthetic conditions are typical for the synthesis of minerals.[51,52] **SION-X** can be obtained under ambient conditions; this is a rare case in which a catalytically active synthetic mineral can be synthesized in a large-scale without the need of high temperature or pressure. Moreover, when the synthesis conditions of Cu-bpy-Cl are considered, the formation of **SION-X** from the MOF is affordable and industrially viable. This synthetic advantage in combination with its self-healing catalytic activity highlights the adequacy of **SION-X** for practical catalytic applications.

Conclusions

In summary, we discovered a novel class of self-healing heterogeneous and sustainable catalyst, **SION-X**, which can efficiently release ~3 equivalents of H_2 from 1 equivalent of AB. It can be easily synthesized, it undergoes reversible metamorphosis and its catalytic activity is not decreased or disabled for at least 10 cycles of reaction. The investigation of **SION-X** introduces a

conceptually new and unique system for heterogeneous catalysis field, which addresses the catalyst deactivation and storage problems in a simple, inexpensive and efficient way. This work highlights that natural minerals, which appear to be benign, under the right conditions, could be transformed into active catalysts that can play a key role in energy-related applications. Our findings on **SION-X** pave the way of a new area of catalysis that explores the development of cheap, sustainable, and easily regenerable catalysts for H_2 generation and other applications.

Conflicts of interest

The authors declare no competing financial interest.

Acknowledgements

K.C.S. and T.N.N. thank Swiss National Science Foundation (SNSF) for funding under the Ambizione Energy Grant No. PZENP2_166888. The authors acknowledge the National Center of Competence in Research (NCCR), Materials' Revolution: Computational Design and Discovery of Novel Materials (MARVEL), of the Swiss National Science Foundation (SNSF) for funding – DD4.5. The authors thank Dr. Pascal Schouwink for the variable temperature PXRD measurements. K.C.S. is thankful to Prof. Paul J. Dyson for his useful comments and discussions.

References

1. S. Kampouri, T. N. Nguyen, C. P. Ireland, B. Valizadeh, F. M. Ebrahim, G. Capano, D. Ongari, A. Mace, N. Guijarro and K. Sivula, *J. Mater. Chem. A*, 2018, **6**, 2476-2481.
2. S.-i. Orimo, Y. Nakamori, J. R. Eliseo, A. Züttel and C. M. Jensen, *Chem. Rev.*, 2007, **107**, 4111-4132.
3. N. L. Rosi, J. Eckert, M. Eddaoudi, D. T. Vodak, J. Kim, M. O'Keeffe and O. M. Yaghi, *Science*, 2003, **300**, 1127-1129.
4. P. Chen, Z. Xiong, J. Luo, J. Lin and K. L. Tan, *Nature*, 2002, **420**, 302.
5. A. Staubitz, A. P. Robertson, M. E. Sloan and I. Manners, *Chem. Rev.*, 2010, **110**, 4023-4078.
6. C. Tang, R. Zhang, W. Lu, L. He, X. Jiang, A. M. Asiri and X. Sun, *Adv. Mater.*, 2017, **29**, 1602441.
7. T. Liu, K. Wang, G. Du, A. M. Asiri and X. Sun, *J. Mater. Chem. A*, 2016, **4**, 13053-13057.
8. A. Staubitz, A. P. Robertson and I. Manners, *Chem. Rev.*, 2010, **110**, 4079-4124.

9. D. F. Schreiber, C. O'Connor, C. Grave, Y. Ortin, H. Müller-Bunz and A. D. Phillips, *ACS Catal.*, 2012, **2**, 2505-2511.
10. U. B. Demirci, *Energy Technol.*, 2018, **6**, 470-486.
11. A. Rossin, G. Tuci, L. Luconi and G. Giambastiani, *ACS Catal.*, 2017, **7**, 5035-5045.
12. Q. Yao, Z.-H. Lu, W. Huang, X. Chen and J. Zhu, *J. Mater. Chem. A*, 2016, **4**, 8579-8583.
13. C. Du, Q. Ao, N. Cao, L. Yang, W. Luo and G. Cheng, *Int. J. Hydrogen Energy*, 2015, **40**, 6180-6187.
14. Q. Yao, Z.-H. Lu, Y. Jia, X. Chen and X. Liu, *Int. J. Hydrogen Energy*, 2015, **40**, 2207-2215.
15. W. Chen, J. Ji, X. Duan, G. Qian, P. Li, X. Zhou, D. Chen and W. Yuan, *Chem. Commun.*, 2014, **50**, 2142-2144.
16. J. Chen, Z.-H. Lu, Y. Wang, X. Chen and L. Zhang, *Int. J. Hydrogen Energy*, 2015, **40**, 4777-4785.
17. Y. Tonbul, S. Akbayrak and S. Özkar, *Int. J. Hydrogen Energy*, 2016, **41**, 11154-11162.
18. M. Kaya, M. Zahmakiran, S. Özkar and M. Volkan, *ACS Appl. Mater. Interfaces*, 2012, **4**, 3866-3873.
19. H.-L. Wang, J.-M. Yan, Z.-L. Wang and Q. Jiang, *Int. J. Hydrogen Energy*, 2012, **37**, 10229-10235.
20. Z.-L. Wang, J.-M. Yan, H.-L. Wang and Q. Jiang, *J. Power Sources*, 2013, **243**, 431-435.
21. J. M. Yan, X. B. Zhang, S. Han, H. Shioyama and Q. Xu, *Angew. Chem. Int. Ed.*, 2008, **47**, 2287-2289.
22. M. Rakap, *J. Alloys Compd.*, 2015, **649**, 1025-1030.
23. X. Li, C. Zeng and G. Fan, *Int. J. Hydrogen Energy*, 2015, **40**, 9217-9224.
24. Q. Yao, K. Yang, X. Hong, X. Chen and Z.-H. Lu, *Catal. Sci. Technol.*, 2018, **8**, 870-877.
25. K. Yang, L. Zhou, X. Xiong, M. Ye, L. Li and Q. Xia, *Microporous Mesoporous Mater.*, 2016, **225**, 1-8.
26. Y. Yamada, K. Yano and S. Fukuzumi, *Energy Environ. Sci.*, 2012, **5**, 5356-5363.
27. C. Y. Peng, L. Kang, S. Cao, Y. Chen, Z. S. Lin and W. F. Fu, *Angew. Chem. Int. Ed.*, 2015, **54**, 15725-15729.
28. C. Tang, L. Xie, K. Wang, G. Du, A. M. Asiri, Y. Luo and X. Sun, *J. Mater. Chem. A*, 2016, **4**, 12407-12410.
29. Z.-C. Fu, Y. Xu, S. L.-F. Chan, W.-W. Wang, F. Li, F. Liang, Y. Chen, Z.-S. Lin, W.-F. Fu and C.-M. Che, *Chem. Commun.*, 2017, **53**, 705-708.
30. C. Tang, F. Qu, A. M. Asiri, Y. Luo and X. Sun, *Inorg. Chem. Front.*, 2017, **4**, 659-662.
31. M. C. Denney, V. Pons, T. J. Hebden, D. M. Heinekey and K. I. Goldberg, *J. Am. Chem. Soc.*, 2006, **128**, 12048-12049.
32. S. Campisi, M. Schiavoni, C. Chan-Thaw and A. Villa, *Catalysts*, 2016, **6**, 185.
33. M. M. Najafpour, M. Fekete, D. J. Sedigh, E.-M. Aro, R. Carpentier, J. J. Eaton-Rye, H. Nishihara, J.-R. Shen, S. I. Allakhverdiev and L. Spiccia, *ACS Catal.*, 2015, **5**, 1499-1512.
34. M. Argyle and C. Bartholomew, *Catalysts*, 2015, **5**, 145-269.
35. A. R. Kampf and G. Favreau, *Eur. J. Mineral.*, 2004, **16**, 361-366.
36. O. Yaghi and G. Li, *Angew. Chem. Int. Ed. Engl.*, 1995, **34**, 207-209.
37. S. R. Batten, J. C. Jeffery and M. D. Ward, *Inorg. Chim. Acta*, 1999, **292**, 231-237.
38. M. Rakap, E. E. Kalu and S. Özkar, *Int. J. Hydrogen Energy*, 2011, **36**, 254-261.
39. M. Rakap and S. Özkar, *Int. J. Hydrogen Energy*, 2011, **36**, 7019-7027.
40. Y. Li, L. Xie, Y. Li, J. Zheng and X. Li, *Chem. Eur. J.*, 2009, **15**, 8951-8954.
41. S. B. Kalidindi, U. Sanyal and B. R. Jagirdar, *Phys. Chem. Chem. Phys.*, 2008, **10**, 5870-5874.

42. D. Tahir and S. Tougaard, *J. Phys.: Condens. Matter*, 2012, **24**, 175002.
43. K. Rajesh, B. Ajitha, Y. A. K. Reddy, Y. Suneetha and P. S. Reddy, *Mater. Today*, 2016, **3**, 1985-1991.
44. K. Guo, H. Li and Z. Yu, *ACS Appl. Mater. Interfaces*, 2018, **10**, 517-525.
45. Q. Yao, Z.-H. Lu, Y. Yang, Y. Chen, X. Chen and H.-L. Jiang, *Nano Res.*, 2018, **11**, 4412-4422.
46. H. Behm and C. Baerlocher, *Acta Crystallogr. Sect. C: Cryst. Struct. Commun.*, 1985, **41**, 5-7.
47. Q. Xu and M. Chandra, *J. Power Sources*, 2006, **163**, 364-370.
48. K. Feng, J. Zhong, B. Zhao, H. Zhang, L. Xu, X. Sun and S. T. Lee, *Angew. Chem. Int. Ed.*, 2016, **55**, 11950-11954.
49. M. W. Kanan and D. G. Nocera, *Science*, 2008, **321**, 1072-1075.
50. C. Costentin and D. G. Nocera, *Proc. Natl. Acad. Sci.*, 2017, **114**, 13380-13384.
51. B. Konkena, K. Junge Puring, I. Sinev, S. Piontek, O. Khavryuchenko, J. P. Dürholt, R. Schmid, H. Tüysüz, M. Muhler and W. Schuhmann, *Nat. Commun.*, 2016, **7**, 12269.
52. S. A. Kondrat, P. J. Smith, P. P. Wells, P. A. Chater, J. H. Carter, D. J. Morgan, E. M. Fiordaliso, J. B. Wagner, T. E. Davies and L. Lu, *Nature*, 2016, **531**, 83.